Supporting Information for

ORIGINAL ARTICLE

Bilayer hydrogel dressing with lysozyme-enhanced photothermal therapy for biofilm eradication and accelerated chronic wound repair

Yizhen Wang[a,†], Qijun Lv[a,†], You Chen[b], Langtao Xu[b], Miao Feng[b], Zhiyong Xiong[a], Jiajun Li[a], Jie Ren[c,*], Jie Liu[b,*], Bo Liu[a,*]

[a]*Department of General Surgery, the Third Affiliated Hospital of Sun Yat-sen University, Guangzhou 510630, China*

[b]*School of Biomedical Engineering, Sun Yat-sen University, Guangzhou 510006, China*

[c]*Department of Ultrasound, the Third Affiliated Hospital of Sun Yat-sen University, Guangzhou 510630, China*

Received 29 January 2022; received in revised form 24 February 2022; accepted 15 March 2022

*Corresponding authors. Tel./fax: +86 20 82179243 (Jie Ren); +86 20 39332145 (Jie Liu); +86 20 82179742 (Bo Liu).

E-mail addresses: renj@mail.sysu.edu.cn (Jie Ren), liujie56@mail.sysu.edu.cn (Jie Liu), liubo3@mail.sysu.edu.cn (Bo Liu).

[†]These authors made equal contributions to this work.

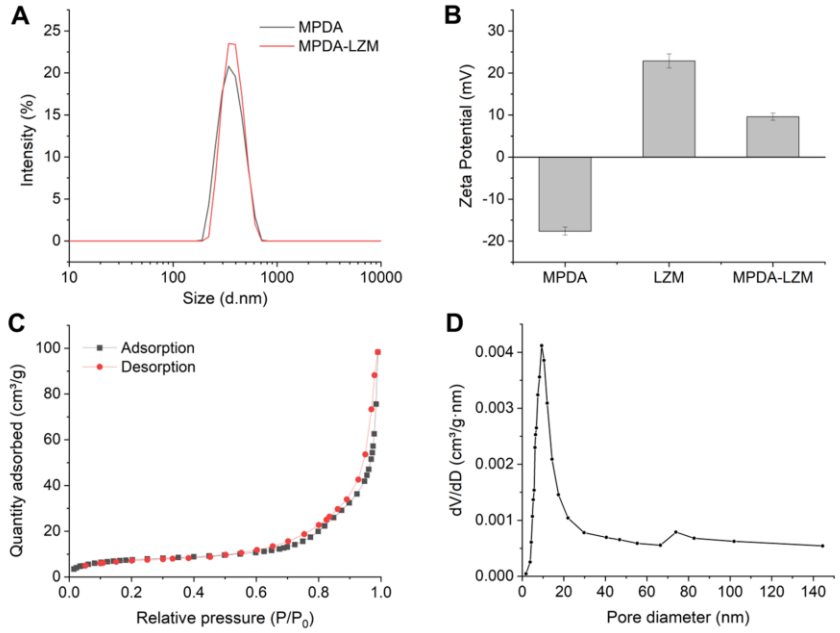

Figure S1 (A) Hydrodynamic size distributions of MPDA nanoparticles and MPDA-LZM nanoparticles. (B) Zeta potentials of MPDA, LZM, and MPDA-LZM (n=3). (C) N_2 adsorption-desorption isotherms and (D) pore size distribution of MPDA nanoparticles.

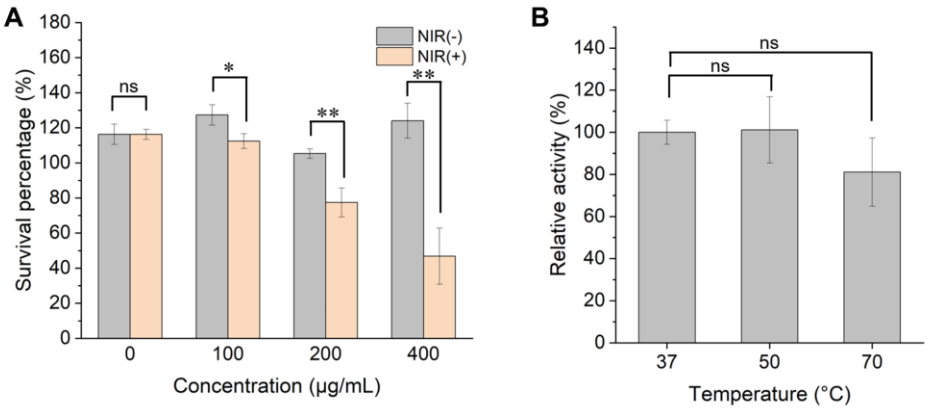

Figure S2 (A) Survival percentages of *E. coli* treated with different concentrations of MPDA-LZM nanoparticles (n=3). (B) Relative activity of lysozyme after incubation for 2 h at different temperatures (37, 50 and 70 ℃) (n=3, *P < 0.05, **P < 0.01, ns: not significant).

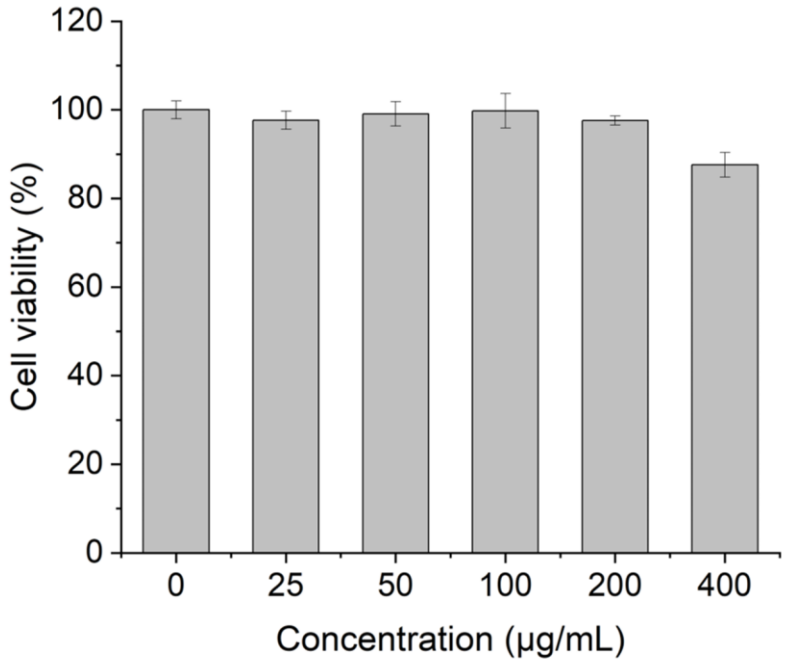

Figure S3 Cell viability of NIH-3T3 cells treated with different concentrations of MPDA-LZM nanoparticles (*n*=3).

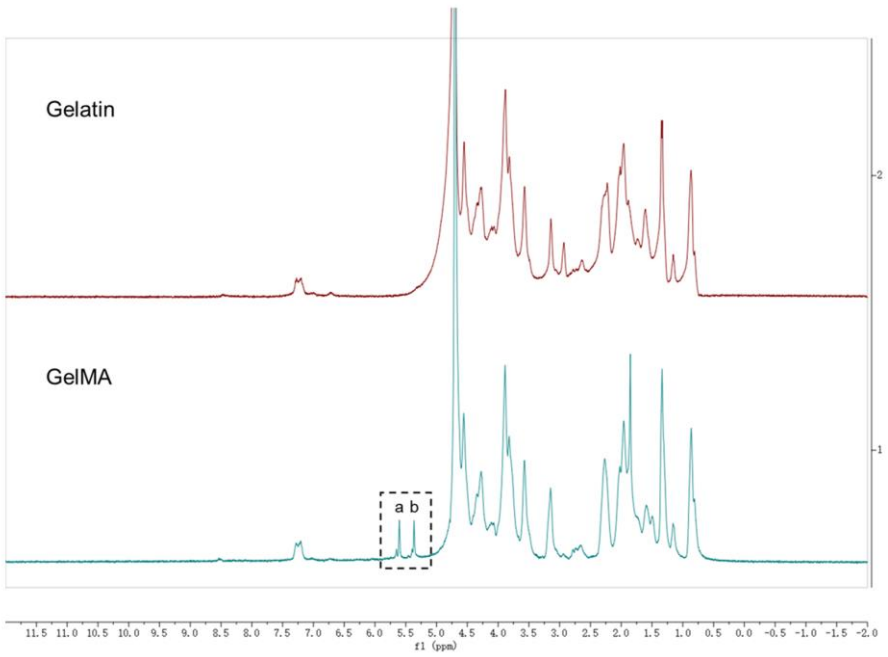

Figure S4 ^{1}H-NMR spectra of gelatin and GelMA. The characteristic peaks of GelMA were labelled as *a* and *b*.

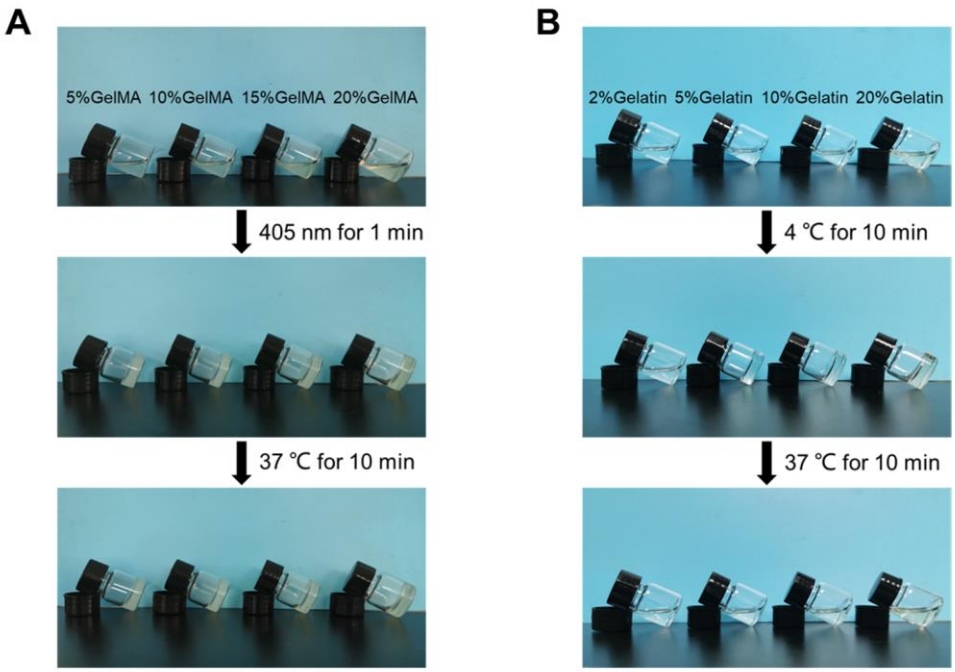

Figure S5 (A) Photographs of the photo-crosslinking process of different concentrations of GelMA. (B) Photographs of the thermo-reversible gel-sol transition of different concentrations of gelatin.

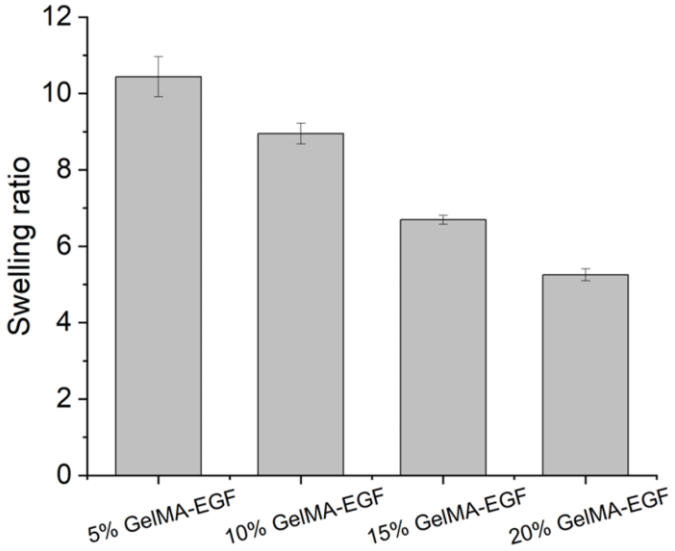

Figure S6 Swelling ratio of GelMA-EGF hydrogel with different concentrations of GelMA (*n*=3).

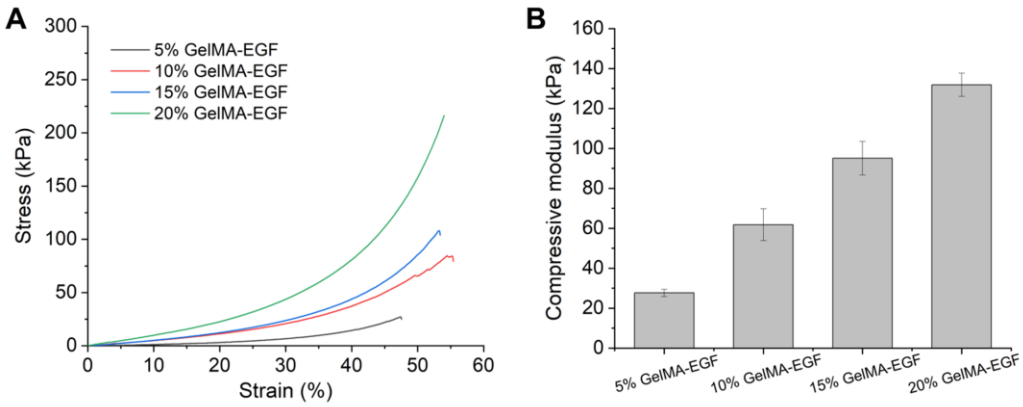

Figure S7 (A,B) Compressive stress-strain curves and compressive modulus of GelMA-EGF hydrogel with different concentrations of GelMA (*n*=3).

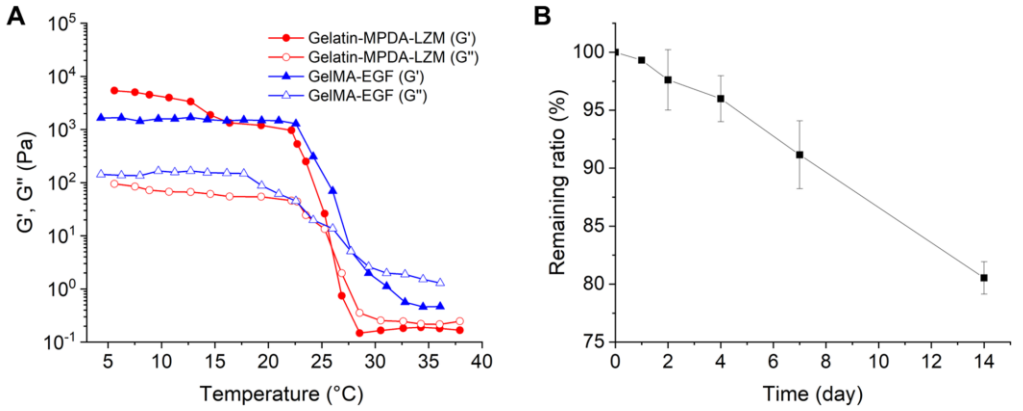

Figure S8 (A) Rheological properties of different hydrogel dependent on temperature. (B) Degradation behavior of GelMA-EGF hydrogel (*n*=3).

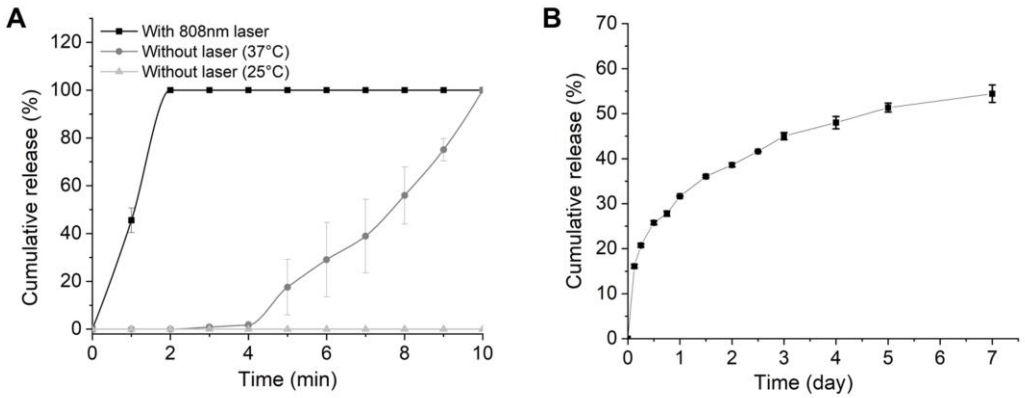

Figure S9 Release curves of (A) MPDA-LZM nanoparticles and (B) EGF loaded in GelMA-EGF/Gelatin-MPDA-LZM bilayer hydrogel (*n*=3).

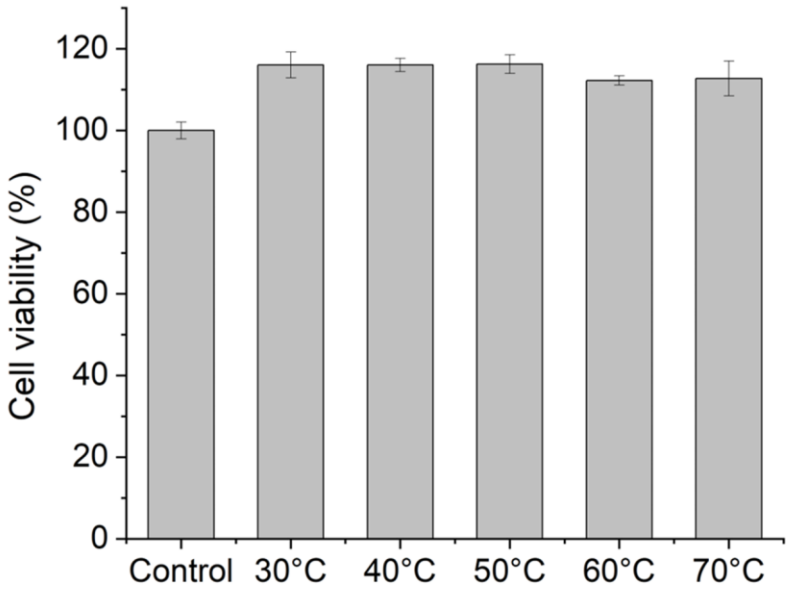

Figure S10 Cell viability of NIH-3T3 cells treated with different temperature pre-treated EGF (*n*=3).

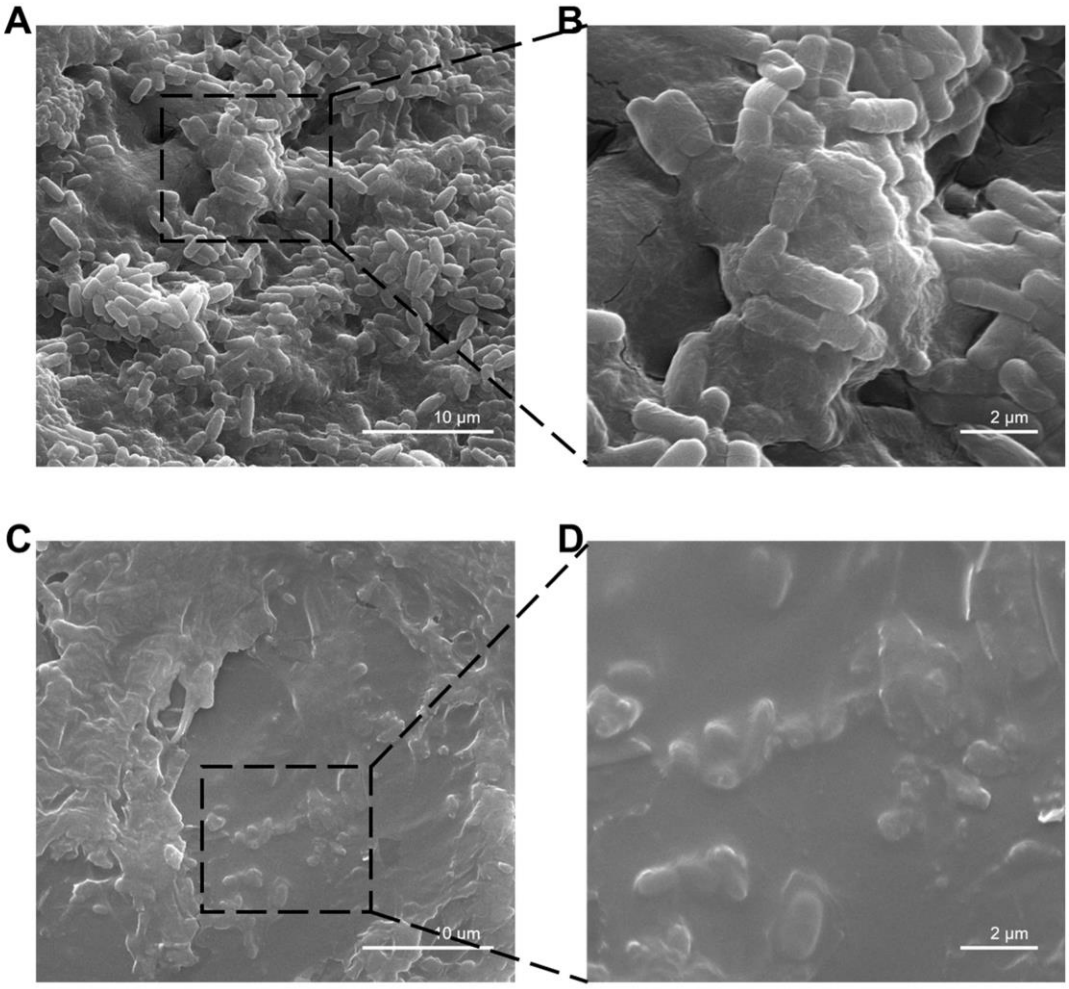

Figure S11 (A,B) SEM images of wound tissues before PTT (scale bar: 10 μm; 2 μm). (C,D) SEM images of wound tissues after PTT (scale bar: 10 μm; 2 μm).

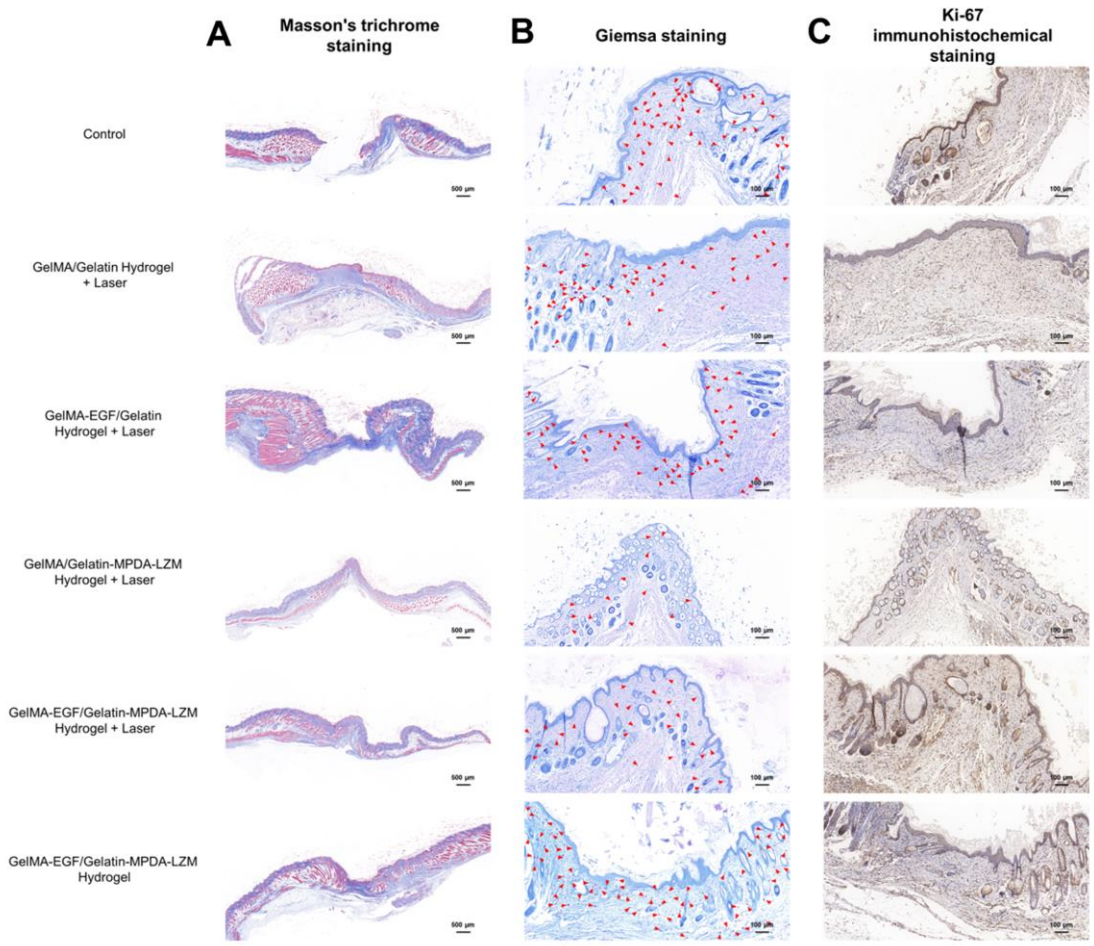

Figure S12 (A) Representative Masson's trichrome staining images and (B) Giemsa staining images of wound skin tissues (scale bar: 500 μm for Masson's trichrome staining, 100 μm for Giemsa staining). Red arrows represent bacteria. (C) Immunohistochemical staining images of Ki-67 in wound tissues (scale bar: 100 μm).